JOURNAL OF
REINFORCED
PLASTICS &
COMPOSITES

Original article

Journal of Reinforced Plastics and Composites
0(0) 1–14

DOI: 10.1177/0731684418808894
journals.sagepub.com/home/jrp
SAGE

The energy absorption enhancement in aramid fiber-reinforced poly (benzoxazine-co-urethane) composite armors under ballistic impacts

Manunya Okhawilai[1], Tewarak Parnklang[1], Phattarin Mora[1], Salim Hiziroglu[2] and Sarawut Rimdusit[1]

Abstract

Energy absorptions under ballistic impacts of aramid fiber-reinforced poly(benzoxazine-co-urethane) composites at urethane mass concentrations of 0, 10, 20, 30, and 40 wt.% were investigated. The energy absorption of the composite was investigated by subjecting eight plies of the specimen with 9 mm and .44 Magnum according to levels II and IIIA of the National Institute of Justice standard-0101.04. The composite having the urethane mass concentration of 20 wt.% exhibited the synergistic behavior in energy absorption at both levels II and IIIA. The 20 wt.% of PU composite also possessed the greatest tensile strength and modulus. The numerical prediction revealed that the ballistic limit of aramid fiber-reinforced poly(benzoxazine-co-urethane) ballistic panel was as high as 690 m s^{-1}. High energy absorption capabilities of the composites can be tailored for fabricating the ballistic panels in soft armor applications.

Keywords

Polybenzoxazine, polyurethane, energy absorption, ballistic impact

Introduction

Energy absorptions of materials are one of the main parameters for assessing and evaluating the armor's performance to withstand the penetration of projectile during the impact incident. Among high-performance ballistic fibers, e.g. ultra-high molecular weight polyethylene (UHMWPE), aramid fibers (Kevlar^{TM} and Twaron^{TM}) and carbon fibers, aramid fibers provide relatively high-specific energy absorptions, and thus they were commonly employed to manufacture ballistic panels in the body armor.[1,2] High-energy absorption materials have to possess high tensile strengths and elongation at breaks. Materials having high tensile modulus values also promoted lower back face deformations.[3]

Fiber-reinforced polymer composites made of the high-strength fiber-embedded polymer matrixes have been increasingly employed in the light-weight armor manufacturing due to the overall high strength and the stiffness to weight ratio. An incorporation of the polymer matrix offered two essential functions. During an impact event, the yarn's integrity remained intact due to the presence of the polymer matrix as observed by Lee et al. [4] The polymer matrix also reduced the effect of the curvature of the projectile on the penetration in which the damage ability of the projectile to puncture the armor decreased.[3] However, the excessive interaction between the polymer matrix and embedded yarns might hinder the movement of yarns to dissipate the absorbed energy and overall ballistic performance of the composites reduced.[5] Gopinath et al.[3] also found that the strong interactions between the stiff matrix and yarns decreased the deflection of the armor, whereas the deformation area increased. Therefore, the polymer

[1]Department of Chemical Engineering, Faculty of Engineering, Chulalongkorn University, Bangkok, Thailand
[2]Department of Natural Resource Ecology and Management, Oklahoma State University, Stillwater, OK, USA

Corresponding author:
Sarawut Rimdusit, Department of Chemical Engineering, Faculty of Engineering, Chulalongkorn University, Bangkok 10330, Thailand.
Email: sarawut.r@chula.ac.th

matrix with the appropriate degree of flexibility and the felicitous polymer matrix–yarn interactions are cardinal for enhancing the ballistic performances of fiber-reinforced polymer composites.

Various polymer matrices such as epoxy,[6,7] polyester,[8] vinyl ester,[9,10] phenolics[11] and polyvinyl butyral (PVB)-phenolic[12] are generally employed for armor manufacturing. An investigation on the ballistic impact response of such high performance materials was through experimental and numerical tools. Ramadhan et al.[13] have developed composite material based on Kevlar 29/epoxy and aluminum-laminated panels and studied its behaviors under impact loading. Silva et al.[14] investigated the impact response of Kevlar 29/Vinylester panels by a fragment simulating projectile (FSP). The comparison on post-impact damage pattern obtained from the simulation and experimental results was carried out. Rodríguez-Millán et al.[12] have studied the impact response of ballistic helmet based on Kevlar 29/PVB-phenolic by the experimental work and with the help of simulation method. The developed numerical model showed high accuracy as the results from those two techniques were equivalent. The ballistic limit value of the material to withstand the penetration of .22 caliber FSP was reported to be 686.6 m s^{-1}. In this work, benzoxazine resin (BA-a) which is a novel kind of thermosetting phenolic resin was exploited as the polymer matrix. BA-a exhibited a myriad of outstanding characteristics, e.g. straightforward monomer preparation with the solvent-less synthesis technique, thermal-triggered ring-opening polymerization without additional catalysts or curing agents required, no by-product release during polymerization, near-zero volumetric shrinkage upon thermal curing, high thermal stability, excellent mechanical properties, low melt viscosity, and ability to alloy with various types of resins.[15–18] Poly(BA-a) composites reinforced with aramid fibers provided improved ballistic performance over the epoxy reinforced with aramid fibers with respect to a higher damage area.[19] However, poly (BA-a) having polar functional groups could form substantial interactions to aramid fibers and the ballistic performance of the composites decreased.[19,20] To alleviate this problem, polyurethane (PU) having a long nonpolar hydrocarbon chain was introduced. PU is the most important tough engineering polymers and can be tailored to offer a wide spectrum of properties. They also possess the excellent flexibility. The toughness of BA-a could be enhanced by alloying with PU and the copolymer of polybenzoxazine and PU (poly (BA-a-co-PU)) also showed the synergism in glass transition temperatures (T_g), i.e. T_g of poly(BA-a-co-PU) was higher than 200°C, whereas those of the parent polymers were 165°C for poly(BA-a) and −71°C for PU.[21]

In this research, the soft ballistic armor from polymer composite having a protection level III was developed. Poly(BA-a-co-PU) was employed as the functional polymer matrix for enhancing the ballistic performance in terms of the energy absorptions of aramid fiber-reinforced polymer composites. The aramid fiber–matrix interactions in the composites were optimized through the PU mass concentrations from 0 to 40 wt.%. The tensile properties of the poly (BA-a-co-PU) composites were also characterized. Aramid fiber-reinforced poly(BA-a-co-PU) composites were subjected to the ballistic impacts of 9 mm full metal jacketed (FMJ) at a velocity of 367 ± 9.1 m/s and .44 magnum semi-jacketed hollow point (SJHP) bullets at a velocity of 436 ± 9.1 m/s. Energy absorptions under ballistic impacts, energy dissipation mechanisms, and failure modes of aramid fiber-reinforced poly(BA-a-co-PU) ballistic composites were also numerically investigated using a commercial simulation program (ANSYS AUTODYN) and compared with the experimental results. In addition, the ballistic limit of the poly(BA-a-co-PU) composites was also numerically estimated.

Experimental

Materials and resin preparations

BA-a, urethane prepolymer (PU), and aramid fibers were used to prepare ballistic composites. BA-a resin is based on bisphenol-A, aniline, and para-formaldehyde. Bisphenol A (polycarbonate grade) was supplied by the PTT Phenol Co., Ltd. Para-formaldehyde and aniline were purchased from Merck Company and Panreac Quimica SA Company, respectively. Urethane prepolymer was prepared from toluene diisocyanate (TDI) and polyether polyol. Polyether polyol with a molecular weight of 2000 g mol^{-1} and toluene diisocyanate were obtained from IRPC Public Company Limited. Aramid fibers possessing a plain weave pattern having 3360 dtex (50% ends) in warp and 3360 dtex (50% picks) in weft direction and an areal density of 340 g m^{-2} were employed as reinforcing fibers. Aramid fibers were purchased from Thai Polyadd Limited Partnership.

BA-a was synthesized from bisphenol A, aniline, and paraformaldehyde at a molar ratio of 1:2:4 based on the solvent-less technology.[22] The three reactants were continuously mixed at 110°C for approximately 40 min to yield a light yellow, low viscosity liquid monomer that solidified at room temperature. The obtained solid monomer was pulverized into fine powder and kept in a refrigerator for future use. PU was prepared from toluene diisocyanate and polypropylene glycol (M_w = 2000 g mol^{-1}). The two reactants

were directly mixed and vigorously stirred in a four-necked round-bottomed flask under a nitrogen stream at 60°C for 40 min to yield a light-yellow liquid prepolymer. The molecular structures of BA-a and PU are shown in Figure 1(a) and (b), respectively.

Preparation of polymer matrixes and ballistic panels

The BA-a and PU binary mixture at PU mass concentrations of 0, 10, 20, 30, and 40 wt.% were prepared as functional matrixes for fiber-reinforced ballistic composites. BA-a monomer was thoroughly mixed with PU at 80℃ until a homogeneous mixture of the polymer matrix was obtained. The compositions of the polymer matrix were denoted according to the PU mass concentration of *x*wt.% as follows: poly((100–*x*)BA-a-co-*x*PU). The hand lay-up procedure was employed to fabricate the laminated ballistic panels. Aramid fibers were pre-impregnated with the prepared copolymer matrix at a temperature of 120℃. The weight fraction of the fiber was kept constant at 65–70 wt.%. The prepregs were then molded employing a compression molder at a temperature of 200℃ under a pressure of 10 MPa for 2 h.

Specimen characterization

In order to determine the energy absorptions of aramid fiber-reinforced poly(BA-a-co-PU) specimens at PU mass concentrations of 0, 10, 20, 30, and 40 wt.%, the composite panels with eight plies having dimensions of 150 × 150 × 2.97 mm^3 were manufactured. The ballistic test was performed at Office of Logistics, Royal Thai Police, Bangkok, Thailand. The specimens were mounted on a metal frame. Four sides of the panels were clamped and placed 5 m in line to the gun barrel. The ballistic tests of the composite panels were performed at the center of the panels by impacting with 9 mm FMJ projectiles at a velocity of 367 ± 9.1 m s^{-1} and .44 Magnum SJHP bullets at a velocity of 436 ± 9.1 m s^{-1} according to NIJ Standard-0101.04 at protection levels II and IIIA, respectively.[23] The ballistic test setup as suggested by NIJ is shown in Figure 2. The setup mainly consisted of a gun barrel, a specimen holder and two sets of chronographs which were used to determine the velocity of the bullet by measuring the time of bullet travelling through the distance of chronograph. The first chronograph in front of the specimen was employed to measure the impact velocity of the bullet before impacting the specimen. The other chronograph was placed behind the specimen to measure the residual velocity of the bullet after penetrating the specimen. The energy absorption by the composite specimen was determined by the difference of an initial kinetic energy and a final kinetic energy according to equation (1)

$$E_a = \frac{1}{2} m_j V_s^2 - \frac{1}{2} m_j V_r^2 \quad (1)$$

where E_a is the energy of absorption (J). m_j is the mass of a projectile (g). V_s and V_r are striking and residual velocities (m s^{-1}), respectively. It should be noted that

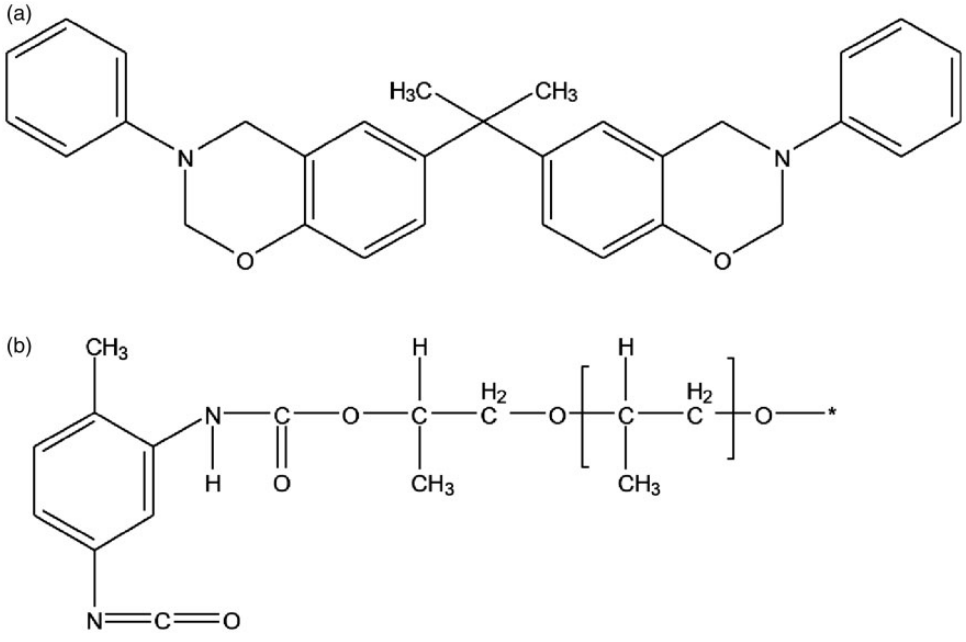

Figure 1. (a) Bisphenol A-based benzoxazine monomer (b) TDI and polypropylene glycol-based urethane prepolymer. TDI: toluene diisocyanate.

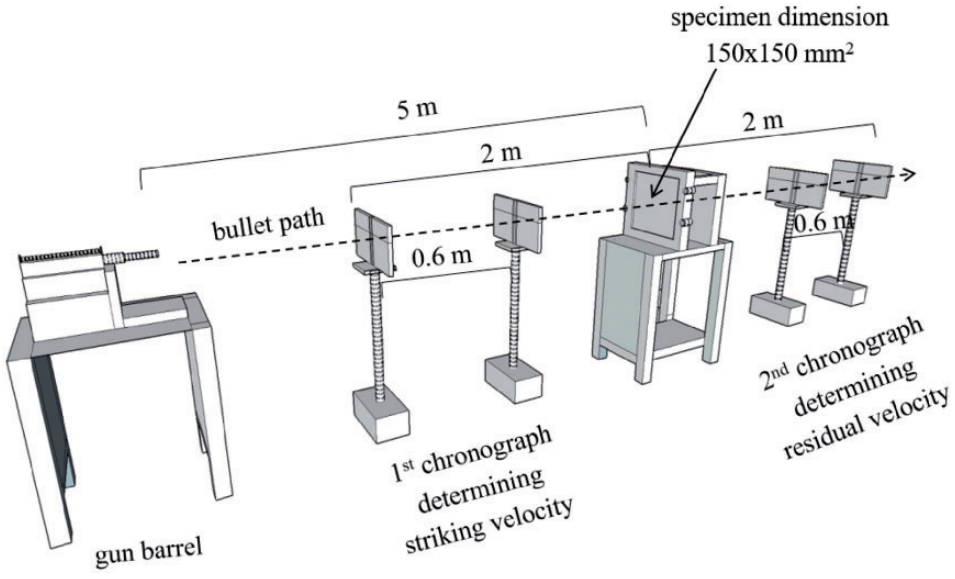

Figure 2. The ballistic test setup with two sets of chronographs to determine striking and residual velocities of projectiles.

a non-fragmented projectile and the conservation of energy are assumed for this measurement.

To illustrate the ballistic performance enhancement of the functional polymer matrix, the neat aramid fabric having the same dimensions as aramid fiber reinforced poly(BA-a-co-PU) was prepared and subjected to a .44 Magnum SJHP bullets at a velocity of 436 $\pm$ 9.1 m s^{-1} at the protection level of IIIA. The bulge formation and damage area of those panels were compared.

The tensile test of the eight plies samples was carried out according to ASTM D3039 using a universal testing machine, Instron model 5567. The total length, gauge length, and the thickness of the specimens were 150, 70 and 3 mm, respectively. A constant cross-head speed for the test was 2 mm min^{-1}. The reported tensile strength, the modulus, and the elongation at break values of the specimens were averaged from five repetitive measurements.

Computational studies on the ballistic behavior of the composites

The ballistic performance of aramid fiber-reinforced poly(BA-a-co-PU) ballistic panels was evaluated numerically with a commercial ANSYS AUTODYN. Aramid fiber-reinforced poly(BA-a-co-PU) composite was simulated as the orthotropic material in which the material properties differ along the three orthogonal planes. In ANSYS AUTODYN, the orthotropic equation of state (EOS) allows a nonlinear EOS to be used in coupled with an orthotropic stiffness matrix. The composite laminates reinforced with aramid fabrics having a plain weave pattern were assumed to have identical properties in the fiber directions but different properties from each other through the thickness direction. It was also assumed that materials were homogeneous. Four edges of the panels were constrained for the movement. An initiation of failure resulted from the excessive tensile or shear stress and/or strain.

A 9 mm FMJ projectile made of a copper jacket with a lead core was modeled following the strength models of Steinberg-Guinan. The material properties of the projectile were obtained from the standard ANSYS AUTODYN material library as shown in Table 1.[24] The geometry of the projectile, the composite panel, and the mesh creation are shown in Figure 3. The simulation was performed under the same conditions as in the experimental work to have an accurate comparison. In order to validate the input properties of the materials, the deformation of the panel observed from the experimental and numerical results was compared as this procedure was widely used for material properties validation.[13,25] Moreover, energy absorptions of 8-ply poly(80BA-a-co-20PU) composite panels having dimensions of 150 $\times$ 150 $\times$ 2.97 mm^3 were numerically predicted and compared with the values from ballistic impact experiments. The 8-ply of the specimens was employed to ensure the perforation so that the residual velocity of the projectile can be measured. The failure characteristics, deformation patterns, and energy dissipation mechanisms of the ballistic panel were deduced from the simulated ballistic impacts.

The ballistic limit of the composite system based on NIJ protection level IIIA was numerically estimated

Table 1. Material properties for 9 mm projectile.[24]

Material: Lead core	Value	Property	Value
Density	11,340 Kg m^{-1}	Equation of state	Shock EOS linear
Shear modulus	8600 MPa	Gruneisen coefficient	2.74
Plasticity	Steinberg Guinan strength	Parameter C1	2006 m s^{-1}
Initial yield stress	8 MPa	Parameter S1	1.429
Maximum yield stress	100 MPa	Parameter quadratic S2	0 s m^{-1}
Hardening constant	110	Failure	
Hardening exponent	0.052	Maximum equivalent plastic strain	2
Derivative dG/dP	1		
Derivative dG/dT	−9.976 MPa°C^{-1}		
Derivative dY/dP	0.0009304	Melting temperature	760 K
Material: Copper jacket	Value	Property	Value
Density	8450 kg m^{-1}	Equation of state	Shock EOS linear
Shear modulus	3000 MPa	Gruneisen coefficient	2.04
		Parameter C1	3726 m s^{-1}
		Parameter S1	1.434

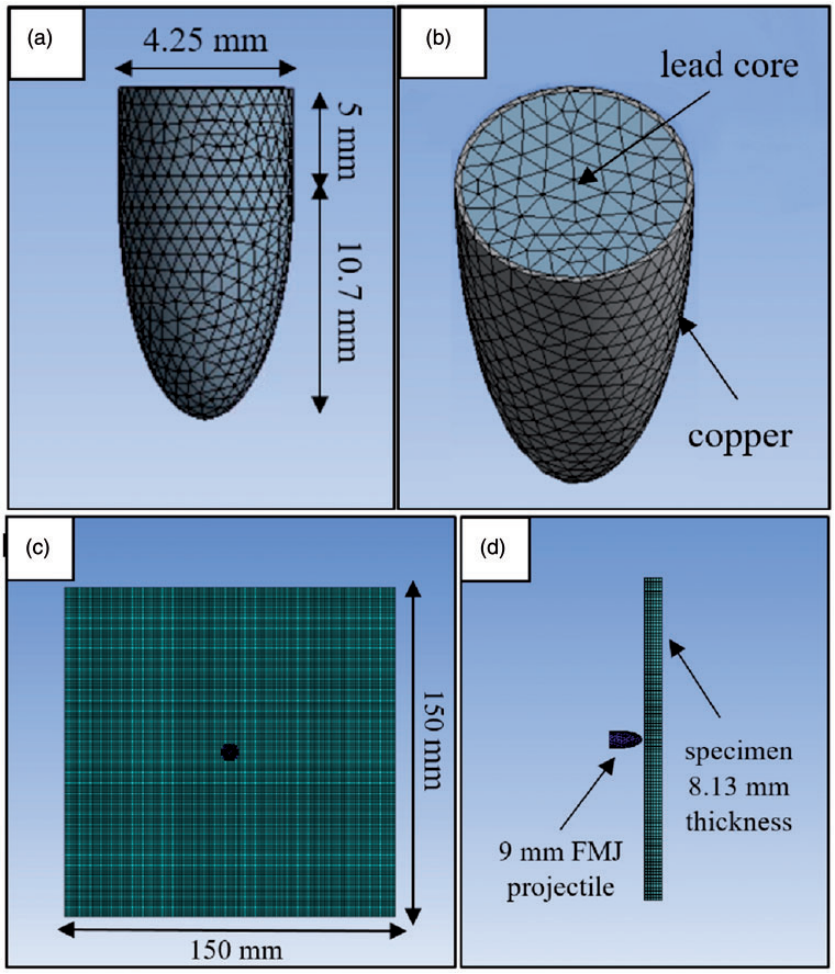

Figure 3. (a) The mesh formation of a copper jacket and (b) a lead core of a 9 mm FMJ bullet (c) Front view and (d) side view of the aramid fiber-reinforced poly(80BA-a-co-20PU) panel.
FMJ: full metal jacketed.

Table 2. Energy absorption abilities of aramid fiber-reinforced poly(BA-a-co-PU) composites at various PU mass concentrations according to the NIJ protection level II.

Mass ratio of poly(BA-a-co-PU)	Sample number	Impact velocity ($m\ s^{-1}$)	Residual velocity ($m\ s^{-1}$)	Impact energy (J)	Residual energy (J)	Energy absorption (J)	Ave. energy absorption (J)	Ave. energy absorption/ thickness ($J\ mm^{-1}$)
100-co-0	1	358.08	327.30	789.20	659.36	129.85	106.68±24.77	37.17±8.86
	2	365.59	340.36	822.65	713.03	109.63		
	3	360.11	341.45	798.18	717.60	80.58		
90-co-10	1	375.75	345.21	869.01	733.49	135.52	130.69±5.35	45.43±0.91
	2	380.62	352.95	891.68	766.75	124.93		
	3	376.14	346.55	670.82	739.20	131.62		
80-co-20	1	364.76	333.15	818.92	683.14	135.79	135.5±8.26	48.39±2.95
	2	357.11	322.79	784.93	641.31	143.62		
	3	362.50	332.80	808.81	681.70	127.10		
70-co-30	1	356.32	332.11	781.46	682.40	99.06	116.16±18.05	40.20±5.86
	2	360.97	329.18	801.99	666.95	135.04		
	3	357.14	330.10	785.06	670.69	114.38		
60-co-40	1	355.88	330.18	779.53	671.01	108.52	122.95±13.56	42.54±5.26
	2	363.07	333.96	811.35	686.46	124.89		
	3	354.68	322.17	774.29	638.85	135.44		

PU: polyurethane.

from the 25-ply ballistic panel having dimensions of $150 \times 150 \times 8.13\ mm^3$. The aramid fiber-reinforced poly(BA-a-co-PU) ballistic panel having the optimum ballistic performance was employed. The specimen dimensions resembled the ballistic panel utilized in the actual light weight body armor. The failure characteristics and deformation patterns of the ballistic panel were deduced from the simulated ballistic impacts. The ballistic limit was determined by varying impact velocities of the projectile until the sample was perforated. The reported value was the maximum impact velocity of the projectile in which the ballistic panel was partially penetrated.

Results and discussion

The energy absorption ability of aramid fiber-reinforced poly(BA-a-co-PU) composites

The energy absorptions of aramid fiber-reinforced poly (BA-a-co-PU) composites having eight plies with various PU mass concentrations from 0 to 40 wt.% were evaluated. The composite panels were subjected to the complete penetration by 9 mm FMJ bullets at velocities of $367 \pm 9.1\ m\ s^{-1}$ according to NIJ Standard-0101.04 at the ballistic protection levels II. At the protection level II, the energy absorptions increased from 106.7 ± 24.8 J of poly (100BA-a-co-0PU) composite reinforced with aramid fibers to 130.7 ± 5.4 and 135.5 ± 8.3 J of the aramid fiber-reinforced poly(90BA-a-co-10PU) and poly(80BA-a-co-20PU) composites, respectively (Table 2). The favorable effect of PU in aramid fiber-reinforced poly(BA-a-co-PU) composites was clearly evidenced. The enhancement in the energy absorption of the poly(80BA-a-co-20PU) composite specimen was ~27% greater than the energy absorption of the poly(100BA-a-co-0PU) specimen. For poly (70BA-a-co-30PU) and poly(60BA-a-co-40PU) composites reinforced with aramid fibers, the energy absorptions reduced to 116.6 ± 26.1 and 123.0 ± 13.6 J which accounted to be 9% and 16% greater than that of poly (100BA-a-co-0PU), respectively. The maximum synergistic effect in the energy absorption was observed at the composite specimen with the PU mass concentration of 20 wt.%. A considerably strong interfacial adhesion between the pure poly(BA-a) and aramid fiber was formed as previously reported.[16] It was attributed to the formation of the polar interaction between carboxyl and ether groups of aramid fibers and hydroxyl groups of the pure poly(BA-a).[26] Therefore, the projectiles could penetrate easily and the fiber failure was dominant. Aramid fiber-reinforced poly(70BA-a-co-30PU) and poly(60BA-a-co-40PU) composite specimens delaminated more readily and excessively due to their weak adhesion interaction. Consequently, less energy absorptions by the composites were observed. In the latter case, the delamination of the composite laminates was a major failure mechanism.

Nayak et al.[5] reported that the weak fiber-matrix adhesion is advantageous for ballistic applications. Weak adhesion facilitated the effortless debonding of fibers from the matrix and resulted in an additional

Table 3. Energy absorption abilities of aramid fiber-reinforced poly(BA-a-co-PU) composites at various PU mass concentrations according to the NIJ protection level IIIA.

Mass ratio of poly(BA-a-co-PU)	Sample number	Impact velocity ($m\ s^{-1}$)	Residual velocity ($m\ s^{-1}$)	Impact energy (J)	Residual energy (J)	Energy absorption (J)	Ave. energy absorption (J)	Ave. energy absorption/ thickness ($J\ mm^{-1}$)
100-co-0	1	422.18	383.13	2160.22	1779.08	381.14	355.77±24.11	120.85±7.36
	2	424.16	388.31	2180.53	1827.51	353.02		
	3	419.98	385.87	2137.76	1804.62	333.15		
90-co-10	1	430.13	387.56	2242.34	1820.45	421.88	392.9±14.2	138.8±4.7
	2	424.09	386.57	2179.81	1811.16	368.64		
	3	420.01	380.09	2137.96	1750.95	387.01		
80-co-20	1	424.68	382.87	2185.88	1776.66	409.22	399.83±10.13	148.08±3.75
	2	424.66	385.01	2185.67	1796.58	389.09		
	3	425.10	384.20	2190.21	1789.03	401.18		
70-co-30	1	418.98	379.68	2127.60	1747.18	380.41	378.95±17.52	130.52±6.03
	2	417.82	376.73	2115.83	1720.14	395.69		
	3	416.01	378.55	2097.54	1736.80	360.74		
60-co-40	1	413.98	375.11	2073.69	1702.56	371.13	366.40±19.51	131.48±9.95
	2	425.00	390.08	2189.18	1844.21	344.97		
	3	423.48	384.35	2173.54	1790.43	383.12		

PU: polyurethane.

energy absorption mechanism through the fiber pull-out.[5] The results from our ballistic test of the aramid fiber-reinforced poly(80BA-a-co-20PU) composite revealed that an appropriate adhesion between the poly(BA-a-co-PU) matrix and the reinforcing aramid fibers provided an enhancement in the ballistic performance as a result from the synergistic energy absorption.

The ballistic performance of aramid fiber-reinforced poly(BA-a-co-PU) specimens at the PU mass concentrations of 0–40 wt.% was also evaluated at the NIJ ballistic protection level IIIA as displayed in Table 3. The composite panels were impacted by .44 Magnum SJHP bullets with the velocities of $436 \pm 9.1\ m\ s^{-1}$. The energy absorption of the aramid fiber-reinforced poly (100BA-a-co-0PU) composite was 355.7 ± 24.1 J. With an addition of 10 and 20 wt.% of the PU, the values increased to 392.9 ± 14.2 and 399.83 ± 10.13 J, respectively. When PU mass concentrations of 30 and 40 wt. % were employed, the energy absorption values dropped to 379.0 ± 17.5 and 366.4 ± 19.5 J, respectively. From the result, the maximum synergy in the energy absorption of the aramid fiber-reinforced poly(80BA-a-co-20PU) composite was observed at the protection level III-A as well as that observed at the protection level II. In comparison to the fiber-reinforced epoxy composite, the energy absorption by the 8-ply aramid fiber-reinforced poly(80BA-a-co-20PU) composite was found to be greater than that of a 16-ply fiber-reinforced epoxy composite (12 plies of aramid/epoxy plus 4 plies of glass fiber/epoxy). The energy absorption of the fiber-reinforced epoxy composite was 369 J, whereas its thickness was 7.6 mm higher than the thickness of the poly(80BA-a-co-20PU) composite.[9] The results suggested that the copolymer of polybenzoxazine and PU could be employed as the ballistic fiber-embedded polymer matrix that provided the better or comparable ballistic performance in terms of the energy absorption when compared to the conventional epoxy resin.

Currently, there has been limited report on utilization of a copolymer as a binder for the development of a ballistic armor. The enhancement on the ballistic protection capability has focused mainly on the development of the hybrid composites,[9,27] the particles with high energy absorption filled in the polymers composites,[28,29] and the honeycomb structures.[30] The energy dissipation of the armor panel could be enhanced effectively by optimizing the adhesions between the polymer matrix and the reinforcing fibers. High-energy absorbing ballistic panels could be potentially employed for a light-weight armor manufacturing since the number of plies and thickness of the panel could be reduced without compromising the ballistic performance. Although aramid fiber reinforced-pure poly(BA-a) composite exhibited the lowest ballistic performance among other aramid fiber-reinforced poly(BA-a-co-PU) composites, Kevlar^{TM}-reinforced poly(BA-a) composites were reported to show a higher energy absorption than the neat bisphenol A-based epoxy composites reinforced with Kevlar^{TM} fibers at the same fiber content. At the complete penetration of the projectiles, the

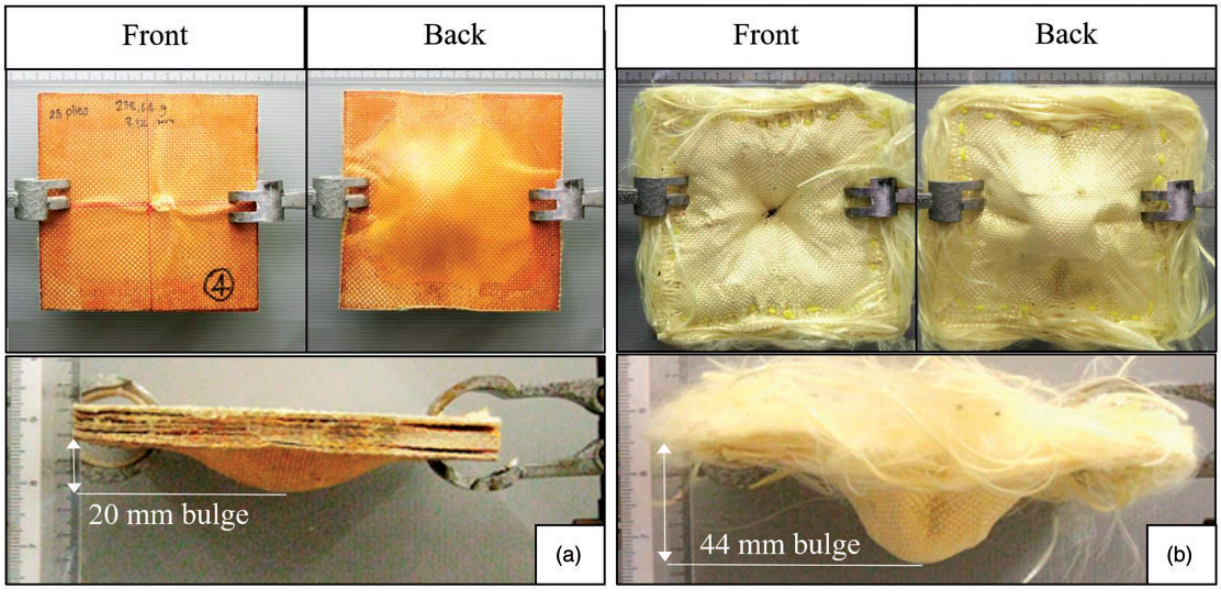

Figure 4. Comparison on the bulge formation of (a) the aramid fiber-reinforced poly(80BA-a-co-20PU) composite and (b) the neat aramid fabric.

pure poly(BA-a) composite showed a larger delaminated area due to a better fiber-matrix delamination process, while a very small delamination was observed in the epoxy composites.[19]

Aramid fabric with various numbers of plies is commercially utilized as an energy absorption panel in a soft body armor to confront a penetration of projectile based on NIJ Standard at test level II-A to IIIA. In this experiment, ballistic performances in terms of perforation resistance and depth of deformation on the back face of aramid fiber-reinforced poly(80BA-a-co-20PU) composite and the neat aramid fabrics at 25 plies were compared. The center of specimens was impacted by .44 Magnum SJHP at the velocities of 436 ± 9.1 m s^{-1}. The deformations of primary yarns by the fibril breakage due to the stretch of fiber by tensile force until exceeding the maximum strength of the composite were obviously noticed on the impact side of the aramid composite, whereas cone formation on the rear side of the aramid composite took place due to the secondary yarn's failure as can be seen in Figure 4. In comparison to the aramid fabric, the aramid composite can maintain its structural integrity with some delamination at the edge of the panel. From back sides of Figure 4(a) and (b), no perforation on both the aramid fiber-reinforced poly(80BA-a-co-20PU) and the aramid fabric was noticed. However, the depth of the bulge observed on the back side of the aramid fiber-reinforced poly(80BA-a-co-20PU) composite (20 mm) after impacted was 45% less than the value of the neat aramid fabric (44 mm). It was attributed to the inter-layer interaction and yarn-to-yarn friction.[31,32] With the presence of poly(BA-a-co-PU) binder, a frictional contact between the projectile and aramid fiber-reinforced poly(80BA-a-co-20PU) composite was higher than that of the neat aramid fabrics. Therefore, the yarn slippage in the aramid fiber-reinforced poly(80BA-a-co-20PU) composite was significantly reduced, resulting in a lower bulge formation depth and a greater structural integrity. Therefore, our findings suggested that the ballistic performance in terms of the trauma depth could be enhanced by 45% by incorporating the poly(80BA-a-co-20PU) matrix to the neat aramid fabrics. Moreover, the damage on the tip of projectile after impacting the specimens was observed as illustrated in Figure 5. It is clearly seen that the aramid composite could destroy the projectile into fragments, indicating that the aramid composite could potentially destroy the tip of projectile. In addition, a classical mushroom shape deformation of the projectile was noticed from the aramid fabric specimen and the projectile impact energy was totally absorbed.

Tensile properties of the aramid fiber-reinforced poly (BA-a-co-PU) composites

The energy absorption by a ballistic panel during an impact of a projectile was attributed to several mechanisms including tensile failures, matrix cracking, delamination, and shear plugging. Tensile failures of primary yarns under an impact point and the surrounding secondary yarns were reported to be the main contributing mechanism for high energy absorptions.[33] Therefore, the tensile properties of the eight plies

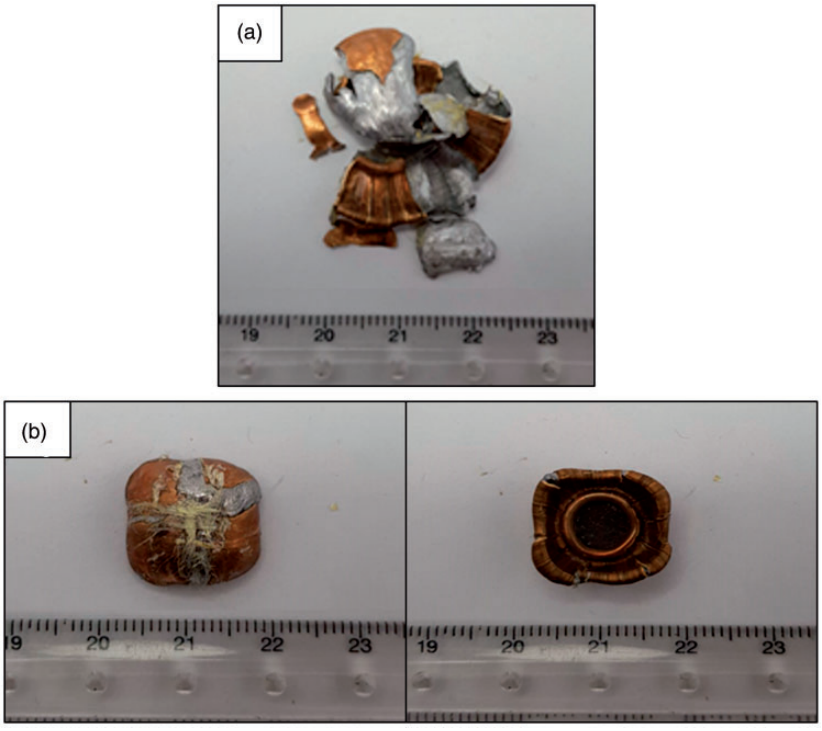

Figure 5. Projectile fragment after penetrated specimens (a) the aramid fiber-reinforced poly(80BA-a-co-20PU) composite and (b) the neat aramid fabric.

Table 4. The tensile properties of the aramid fiber-reinforced poly(BA-a-co-PU) composites at various PU mass concentrations.

Mass ratio of poly(BA-a-co-PU)	Young's modulus (GPa)	Tensile strength (MPa)	Strain at break (%)
100-co-0	11.2±0.8	392.7±34.0	4.7±0.2
90-co-10	17.3±1.1	413.5±22.4	4.5±0.3
80-co-20	22.9±0.5	446.6±48.3	4.3±0.1
70-co-30	20.7±2.2	418.1±41.9	4.3±0.3
60-co-40	16.7±3.4	374.8±34.9	4.7±0.5

PU: polyurethane.

aramid fiber-reinforced poly(BA-a-co-PU) composites were primarily evaluated.

The effect of PU mass concentrations on the tensile properties of the aramid fiber-reinforced poly(BA-a-co-PU) specimen was investigated. The results are shown in Table 4. With an addition of PU in the aramid fiber-reinforced poly(BA-a-co-PU) composites, the modulus values significantly enhanced from 11.2 ± 0.8 GPa of the poly(BA-a) composite to 17.3 ± 1.1 and 22.9 ± 0.5 GPa of the poly(90BA-a-co-10PU) and poly(80BA-a-co-20PU) composites, respectively. The modulus value then slightly decreased to 20.7 ± 2.2 and 16.7 ± 3.4 GPa when the PU mass concentrations in the composite specimens were 30 and 40 wt.%, respectively. The synergistic behavior in the tensile modulus of the aramid fiber-reinforced poly(80BA-a-co-20PU) composite was two times higher than the tensile modulus of the poly (BA-a) composite reinforced with aramid fibers. The synergistic behavior in the flexural modulus of aramid fiber-reinforced poly(80BA-a-co-20PU) having the same number of ply was previously reported by Rimdusit et al.[19] The tensile strength of aramid fiber-reinforced poly(80BA-a-co-20PU) composite (446.6 ± 48.3 MPa) was 54 MPa higher than the tensile strength of the pure poly(BA-a) reinforced with the aramid fibers (392.7 ± 34.0 MPa). The tensile strength of the Kevlar 29/epoxy composite[34] (167.2 MPa) was also lower than the tensile strength of our aramid fiber-reinforced poly(80BA-a-co-20PU) composite at the value of 446.6 ± 48.3 MPa. The aramid fiber-reinforced poly(80BA-a-co-20PU) composites also exhibited greater tensile modulus (22.9 ± 0.5 GPa) and tensile strength (446.6 ± 48.3 MPa) than those of Kevlar/epoxy composite having the values of 12.7 ± 1.1 GPa and 291.1 ± 12.5 MPa, respectively.[35] The results indicated the potential use of our aramid fiber-reinforced poly(80BA-a-co-20PU) as an energy absorption material.

The measured tensile properties of aramid fiber-reinforced poly(BA-a-co-PU) composites were in

Table 5. Materials properties of the aramid fiber-reinforced poly(80BA-a-co-20PU) composite.

Equation of state	Density, g cm^{-3} ρ	Young modulus, kPa E_{11}	E_{22}	E_{33}	Poisson's ratio ν_{12}	ν_{23}	ν_{31}
Orthotropic	1.5	2.3×10^7	2.3×10^7	1.5×10^6	0.07	0.698	0.075
Strength	Shear modulus, kPa			Failure	Tensile failure strain		
	G_{12}	G_{23}	G_{31}		ε_{11}	ε_{22}	ε_{33}
Elastic	3×10^5	1.5×10^4	1.5×10^4	Material stress/strain	0.07	0.07	0.02

agreement with the ballistic performance. The aramid fiber-reinforced poly(80BA-a-co-20PU) composite provided the best ballistic performance and exhibited the synergistic behavior in the ballistic energy absorption, the tensile modulus, and the tensile strength. In addition, the aramid fiber-reinforced poly(80BA-a-co-20PU) demonstrated the conformity between the structural integrity and the ballistic energy absorption. The measured modulus values of the ballistic panel were further employed for numerical investigations.

The comparison on experimental measurements and simulation results of aramid fiber-reinforced poly(BA-a-co-PU) composite panels

An energy absorption of aramid fiber-reinforced poly (80BA-a-co-20PU) was also predicted by a hydrocode simulation and compared to the value determined from the experimental result. The simulation on ballistic test was conducted by impacting a 9 mm FMJ bullet at the velocity of 436 ± 9.1 m s^{-1} for one shot at the center of the 8-ply aramid fiber-reinforced poly(80BA-a-co-20PU) ballistic panel having dimensions of $150 \times 150 \times 2.97$ mm^3. The conditions employed in the numerical investigation were equivalent to the actual experimental setup. The material properties of aramid fiber reinforced poly(80BA-a-co-20PU) composite are presented in Table 5. It was also assumed that the materials were homogeneous. An initiation of failure was triggered from the excessive tensile stress and/or strain or shear stress and/or strain. The predicted energy absorption of the aramid fiber-reinforced poly(80BA-a-co-20PU) composite was 402 J. This value was quite similar to the measured energy absorption of 399 J. The difference was only 0.75%. Therefore, the numerical modeling of the projectile and the ballistic panel and various material parameters utilized in the simulation were validated.

The ballistic panel composed of the 25-ply aramid fiber-reinforced poly(80BA-a-co-20PU) composites was experimentally impacted test. Hence, the ballistic impact on the 25-ply aramid fiber-reinforced poly (80BA-a-co-20PU) composites having dimensions of $150 \times 150 \times 8.13$ mm^3 and areal weight density of 1.067 g cm^{-2} were simulated under the same conditions for the energy absorption prediction. The hole formation and fiber breakages under the impact point and the deformation of primary yarn regions on the impact side of the composite were observed from both the numerical results and the actual experimental measurements as illustrated in Figure 6. These results further corroborated the validation of material parameters employed for the numerical investigations. Therefore, the simulations were additionally exploited for predicting the failure mechanisms of the composite under the ballistic impact and the ballistic limit.

The theoretical investigation on the time-dependent stress distribution and material deformations in the thickness direction during the ballistic impact of the aramid fiber-reinforced poly(80BA-a-co-20PU) are illustrated in Figure 6. At the precise moment of the projectile impact, an exceedingly intense stress around the impact point was generated. The maximum stress recorded at approximately 17 μs was as high as 1×10^5 kPa as indicated by the red region. The radial cone on the back side from fiber failures due to the excessive shear stress and/or strain was subsequently formed as observed in Figure 7(a). At this stage, the deformation of the composite was localized at a limited area. The shape of deformation of the composite panel changed as the projectile penetrates through the specimen at 90 μs. The concentrated stress wave was then propagated along the plane of the panel and through the transverse direction along the panel thickness, resulting in a stretching of the unbroken yarns and a pyramidal shape deformation (by plain weave design of fabric) as noticed in Figure 7(b) and (c). The stress was further propagated and hence the global deformation in the composite was obviously observed (Figure 7(d)).

The ballistic limit and the failure mechanisms of the aramid fiber-reinforced poly(80BA-a-co-20PU) composite panel

The ballistic limit of the 25-ply aramid fiber-reinforced poly(80BA-a-co-20PU) composites with the dimensions of $150 \times 150 \times 8.13$ mm^3 was predicted using the simulation technique by varying an impact velocity

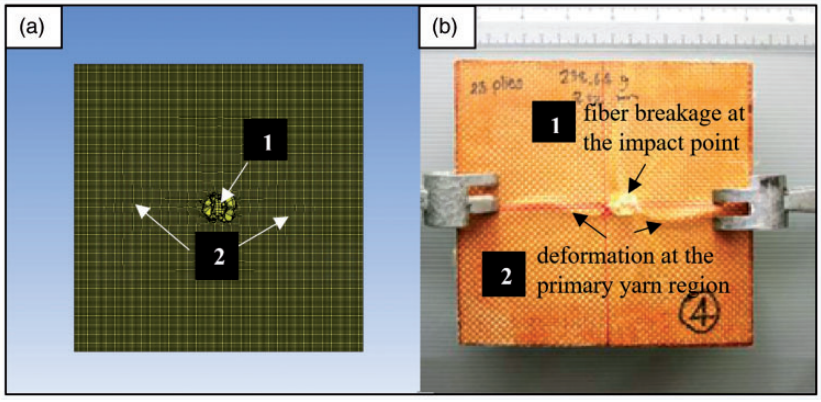

Figure 6. The comparison of the material deformations on the impact side of the 25-ply aramid fiber-reinforced poly(80BA-a-co-20PU) composite panel from (a) the theoretical simulation and (b) the actual experimental measurement.

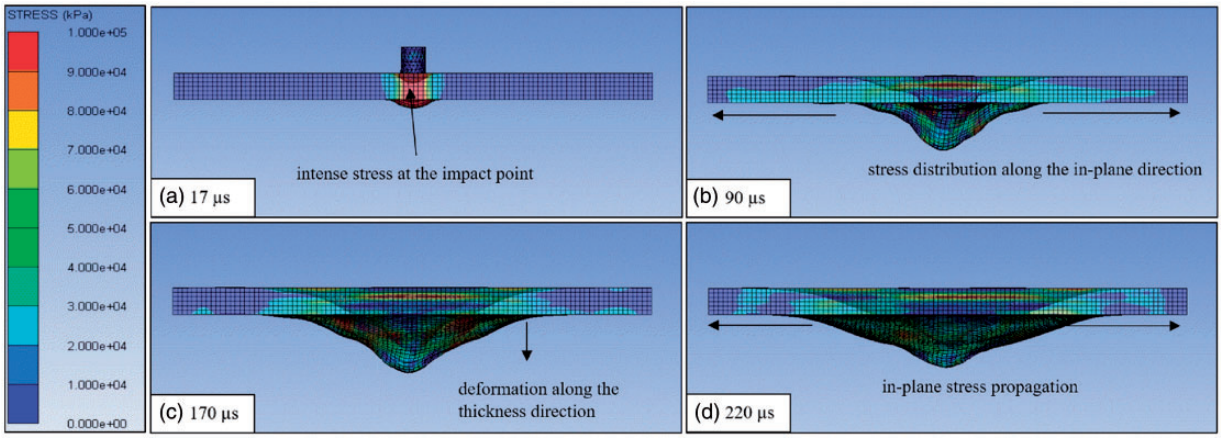

Figure 7. Time-dependent evolutions of the stress distribution and the panel deformations after impacting the 9 mm FMJ projectile onto the 25-ply aramid fiber-reinforced poly(80BA-a-co-20PU) composite.
FMJ: full metal jacketed.

of a 9 mm FMJ bullet until the perforation on the panel was achieved (Figure 8(a)). The predicted ballistic limit of the aramid fiber-reinforced poly(80BA-a-co-20PU) composite panel was determined to be 690 m s^{-1} which was higher than the values of the system summarized in Table 6. Moreover, the ballistic limit of the specimen was experimentally investigated to be greater than 650 m s^{-1}. The projectile velocity higher than 650 m s^{-1} cannot be produced. The high ballistic limit of the aramid fiber reinforced poly(80BA-a-co-20PU) suggested that the poly(BA-a-co-PU) polymer matrixes could be employed to enhance the ballistic performance of fiber-reinforced polymer composites for soft body armor applications.

The failure modes of the 25-ply aramid fiber-reinforced poly(80BA-a-co-20PU) panel impacted by a 9 mm FMJ projectile having an impact velocity of 800 m/s, which exceed the ballistic limit velocity of the sample, obtained from this numerical technique are shown in Figure 8(b). Apparently, the composite panel could not withstand the projectile as noted by the complete penetration. The failure of upper layer of the composite was characterized by stretching and shearing of the fibers adjacent to the impact point which caused a shear plugging of material. The latter layer suffered from stretching and breakage of the primary yarn due to the excessive stress and strain values. At the final stage, the hole deformation observed on the back side of the panel was localized in a limited area. For perforation case, no secondary yarn failure was noticed in contrast to the case of partial penetration where obvious secondary yarn failure was clearly seen (as shown in Figure). Moreover, a stress wave distribution in the in-plane

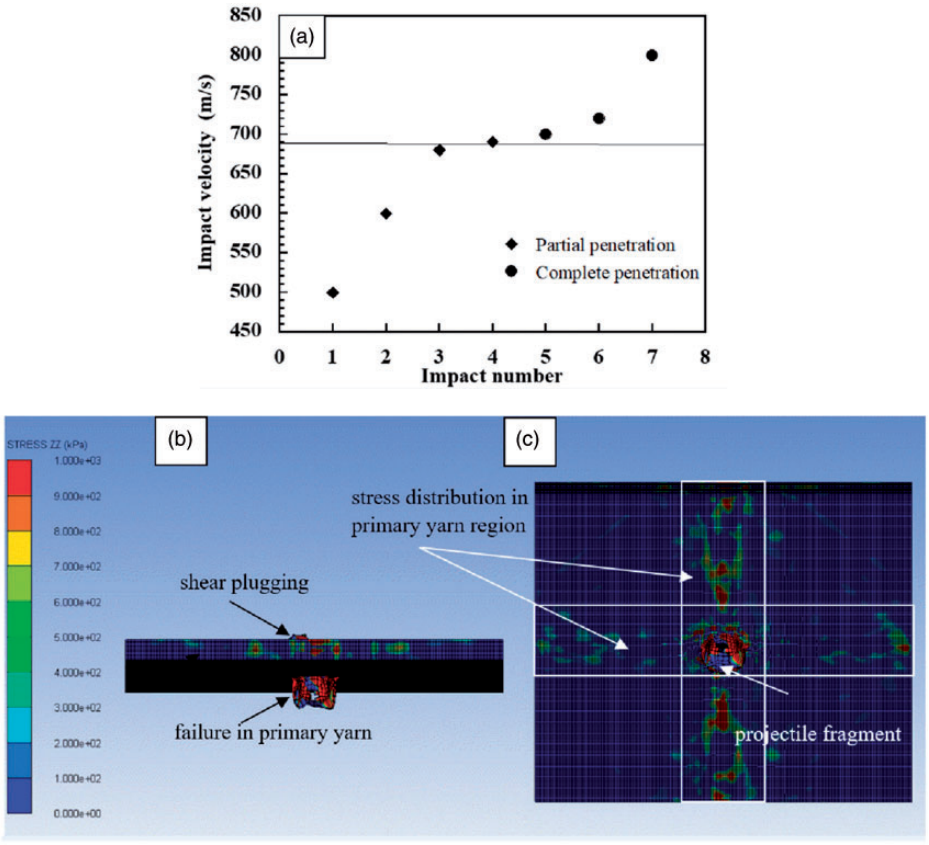

Figure 8. (a) The theoretical ballistic limit determination, (b) the failure mechanisms and (c) the stress distribution of the 25-ply aramid fiber-reinforced poly(80BA-a-co-20PU) composite after subjected to an impact by a 9 mm FMJ projectile having an impact velocity of 800 m/s.
FMJ: full metal jacketed.

Table 6. Comparison on ballistic limit of the present study and some literatures.

Composite system	Thickness (mm)	Projectile	Type of analysis	Ballistic limit (m s^{-1})	Ref.
Aramid fiber reinforced poly(80BA-a-co-20PU) composite	8.13	9 mm FMJ	Numerical	690	This study
3D angle interlock Kevlar/ polypropylene laminate	No data specified	9 mm FMJ	Numerical	470	36
Kevlar® 29/PVB-phenolic	9.5	1.1 g FSP	Numerical	610	37
PVB-phenolic/aramid fiber/kenaf fiber	No data specified	.22 caliber FSP	Numerical	665	38
Kevlar 29/PVB-phenolic	No data specified	.22 caliber FSP	Experimental	686.6	12
Kevlar 29/PVB-phenolic	8 mm	9 mm FMJ	Experimental	680	39

direction on the rear side of the composite panel after penetrated by the projectile was studied as illustrated in Figure 8(c). A much intense stress was located around the perforation region adjacent to the fragment of projectile as the stress value was approximately 1×10^3 kPa. It is also clearly seen that a much lesser stress distribution in the secondary yarn region was formed.

Conclusions

We have successfully demonstrated that the copolymer of polybenzoxazine and PU at the PU mass concentration of 20 wt.% are the effective polymer matrix for enhancing the ballistic performance in terms of the energy absorptions for fiber-reinforced polymer composites. The aramid fiber-reinforced

poly(80BA-a-co-20PU) composite exhibited the synergistic behaviors in the energy absorption according to NIJ Standard-0101.04 at protection levels II and IIIA. In addition, the tensile strength and modulus of the composite formulation exhibited the greatest values of 446.6 ± 48.3 MPa and 22.9 ± 0.5 GPa, respectively. The optimal adhesion of the aramid fiber and the poly (BA-a-co-PU) matrix plays an important role in the synergistic behavior and the ballistic performance of the composite. Three main failure modes including shear plugging, fiber failure and conical deformation were observed in the aramid fiber-reinforced poly (BA-a-co-PU) composites. The energy absorptions, failure modes, and composite deformation mechanisms observed from the experimental results and the simulation results were in good agreement. The numerical ballistic limit of the 25-ply aramid fiber-reinforced poly (80BA-a-co-20PU) specimen was as high as 690 m s^{-1} at the NIJ protection level IIIA. Our results suggested that the appropriate composition of poly(BA-a-co-PU) could enhance ballistic performance of the fiber-reinforced polymer composites so that the aramid fiber-reinforced poly(80BA-a-co-20PU) composite is the promising candidate for ballistic impact resistance applications.

Declaration of conflicting interests

The author(s) declared no potential conflicts of interest with respect to the research, authorship, and/or publication of this article.

Funding

The author(s) disclosed receipt of the following financial support for the research, authorship, and/or publication of this article: The authors would like to express their sincere appreciations to The Royal Golden Jubilee (RGJ) PhD. Program (Grant No.PHD/0030/2554) under the Thailand Research Fund (TRF), Thailand and Chulalongkorn University for the financial support throughout the research. The Ratchadaphiseksomphot Endowment Fund of Chulalongkorn University and the Chulalongkorn Academic Advancement into its 2nd Century Project, Chulalongkorn University are also acknowledged..

References

1. Karahan M, Jabbar A and Karanhan N. Ballistic impact behavior of the aramid and ultra-high molecular weight polyethylene composites. *J Reinf Plast Compos* 2014; 34: 37–48.
2. Millan M, Moreno C, Marco M, et al. Numerical analysis of the ballistic behavior of Kevlar composite under impact of double nosed stepped cylindrical projectiles. *J Reinf Plas Compos* 2015; 35: 124–137.
3. Gopinath G, Zheng JQ and Batra RC. Effect of matrix on ballistic performance of soft body armor. *Compos Struct* 2012; 94: 2690–2696.
4. Lee BL, Walsh TF, Won ST, et al. Penetration failure mechanisms of armor-grade fiber composites under impact. *J Compos Mater* 2016; 35: 1605–1633.
5. Nayak N, Sivaraman P, Banerjee A, et al. Effect of matrix on the ballistic impact of aramid fabric composite laminates by armor piercing projectiles. *Polym Compos* 2012; 33: 443–450.
6. Hosur M, Karim M and Jeelani S. Studies on stitched woven S2 glass/epoxy laminates under low velocity and ballistic impact loading. *J Reinf Plas Compos* 2004; 23: 1313–1323.
7. Kumar S, Gupta D, Singh I, et al. Behavior of Kevlar/epoxy composite plates under ballistic impact. *J Reinf Plast Compos* 2009; 29: 2048–2064.
8. Çallıoğlu H, Sayer M and Demir E. Impact behavior of particles filled-glass/polyester composite plates. *Polym Compos* 2011; 32: 1125–1133.
9. Bandaru AK, Vetiyatil L and Ahmad S. The effect of hybridization on the ballistic impact behavior of hybrid composite armors. *Compos Part B* 2015; 76: 300–319.
10. Grujicic M, Pandurangan B, Angstadt DC, et al. Ballistic-performance optimization of a hybrid carbon-nanotube/E-glass reinforced poly-vinyl-ester-epoxy-matrix composite armor. *J Mater Sci* 2007; 42: 5347–5359.
11. Jordan JB, Naito CJ and Haque BZ. Quasi-static, low-velocity impact and ballistic impact behavior of plain weave E-glass/phenolic composites. *J Compos Mater* 2013; 48: 2505–2516.
12. Rodríguez-Millán M, Ito T, Loya JA, et al. Development of numerical model for ballistic resistance evaluation of combat helmet and experimental validation. *Mater Des* 2016; 110: 391–403.
13. Ramadhan AA, Abu Talib AR, Mohd Rafie AS, et al. High velocity impact response of Kevlar-29/epoxy and 6061-T6 aluminum laminated panels. *Mater Des* 2013; 43: 307–321.
14. Silva MAG, Cismaşiu C and Chiorean CG. Numerical simulation of ballistic impact on composite laminates. *Int J Impact Eng* 2005; 31: 289–306.
15. Rimdusit S, Jubsilp C and Tiptipakorn S. *Alloys and composites of polybenzoxazines*. Singapore: Springer, 2013.
16. Okhawilai M and Rimdusit S. Hard armor composites from ballistic fiber reinforced polybenzoxazine alloys. In: Ishida H and Froimowicz P (ed) *Advanced and emerging polybenzoxazine science and technology*. USA, Elsevier, 2017, pp.699–723.
17. Rimdusit S, Bangsen W and Kasemsiri P. Chemorheology and thermomechanical characteristics of benzoxazine-urethane copolymers. *J Appl Polym Sci* 2011; 121: 3669–3678.
18. Ishida H and Agag T. *Handbook of benzoxazine resin*. Oxford: Elsevier Press, 2012.
19. Rimdusit S, Pathomsap S, Kasemsiri P, et al. Kevlar™ fiber reinforced polybenzoxazine alloys for ballistic impact application. *Eng J* 2011; 15: 23–40.

20. Denchev Z and Dencheva N. Manufacturing and properties of aramid reinforced composites. In: Bhattacharyya SF (ed) *Synthetic polymer-polymer composites*. Munich: Hanser Publishers, 2012, pp.251–280.
21. Rimdusit S, Pirstpindvong S, Tanthapanichakoon W, et al. Toughening of polybenzoxazine by alloying with urethane prepolymer and flexible epoxy: a comparative study. *Polym Eng Sci* 2005; 45: 288–296.
22. Ishida H. Process for preparation of benzoxazine compounds in solventless systems Patent. 5543516, USA, 1996.
23. Samuels JE. U.S. Department of Justice, National Institute of Justice, Ballistic resistance of body armor, NIJ standard 0101.04, 2000.
24. ANSYS AUTODYN Library Version 16. Available at: https://www.ansys.com/products/structures/ansys-autodyn
25. Okhawilai M, HiziroglU S And Rimdusit S. Measurement of ballistic impact performance of fiber reinforced polybenzoxazine/polyurethane composites. *Measurement* 2018; 130: 198–210.
26. Liu L, Huang YD, Zhang ZQ, et al. Ultrasonic treatment of aramid fiber surface and its effect on the interface of aramid/epoxy composites. *Appl Surf Sci* 2008; 254: 2594–2509.
27. Pandya KS, Pothnis JR, Ravikumar G, et al. Ballistic impact behavior of hybrid composites. *Mater Des* 2013; 44: 128–135.
28. Manero A, Gibson J, Freihofer G, et al. Evaluating the effect of nano-particle additives in Kevlar® 29 impact resistant composites. *Compos Sci Technol* 2015; 116: 41–49.
29. Gibson J, McKee J, Freihofer G, et al. Enhancement in ballistic performance of composite hard armor through carbon nanotubes. *Int J Smart Nano Mater* 2013; 4: 212–228.
30. Liaghat GH, Nia AA, Daghyani HR, et al. Ballistic limit evaluation for impact of cylindrical projectiles on honeycomb panels. *Thin Wall Struct* 2010; 55: 48–61.
31. Othman AR and Hassen MH. Effect of different construction designs of aramid fabric on the ballistic performances. *Mater Des* 2013; 44: 407–413.
32. Gu B. Ballistic penetration of conically cylindrical steel projectile into plain-woven fabric target – a finite element simulation penetration of conically cylindrical steel projectile into plain-woven fabric target – a finite element simulation. *J Compos Mater* 2004; 38: 2049–2074.
33. Naik NK. Analysis of woven fabric composites for ballistic protection. In: Chen X (ed) *Advanced fibrous composite materials for ballistic protection*. Kidlington, UK: Woodhead Publishing, 2016, pp.217–262.
34. Reddy AC. Evaluation of Curing Process for Kevlar 49-Epoxy composites by mechanical characterization designed for brake liners. *Int J Sci Res* 2013; 4: 2365–2371.
35. Valenca SL, Griza S, Oliveira VG, et al. Evaluation of the mechanical behavior of epoxy composite reinforced with Kevlar plain fabric and glass-Kevlar hybrid fabric. *Compos Part B* 2015; 70: 1–8.
36. Bandaru AK, Chavan VV, Ahmad S, et al. Ballistic impact response of Kevlar® reinforced thermoplastic composite armors. *Int J Impact Eng* 2016; 89: 1–13.
37. Tham CY, Tan VBC and Lee HP. Ballistic impact of a KEVLAR® helmet: experiment and simulations. *Int J Impact Eng* 2008; 35: 318–304.
38. Salman SD, Leman Z, Sultan MTH, et al. Effect of kenaf fibers on trauma penetration depth and ballistic impact resistance for laminated composites. *Text Res J* 2017; 87: 2051–2065.
39. Colakoglu M, Soykasap O and Özek T. Experimental and numerical investigations on the ballistic performance of polymer matrix composites used in armor design. *Appl Compos Mater* 2007; 14: 47–58.